Effects of Molecular Weight Distribution and Long-Chain Branching on the Viscoelastic Properties of High- and Low-Density Polyethylene Melts

CHANG DAE HAN and CARLOS A. VILLAMIZAR, *Department of Chemical Engineering, Polytechnic Institute of New York, Brooklyn, New York 11201*

Synopsis

Using the Han slit/capillary rheometer, rheological measurements were taken of several commercially available low- and high-density polyethylene melts, namely, three low-density polyethylene samples of Chemplex Corp. (CX 1005, CX 1016, and CX 3020), three low-density polyethylene samples of U.S. Industrial Chemicals Co. (NA 205, NA 244, and NA 279), two high-density polyethylene samples of Union Carbide Corp. (DMDJ 5140 and DMDJ 4306), and two high-density polyethylene samples of Mitsui Petrochemical Industries, LTD. Molecular characterization of these samples was carried out by the resin suppliers. The rheological measurements included (1) entrance pressure drop, (2) exit pressure, (3) pressure gradient, (4) die swell ratio. These then permitted us to determine the shear viscosity and normal stress differences. The rheological measurements were interpreted to identify the effects of long-chain branching and molecular weight distribution on the rheological properties of polyethylenes in the light of the existing molecular viscoelasticity theories. It was found that fluid elasticity is greater for polymers having a broader molecular weight distribution and that, for polymers having more long-chain branching, viscosities are lower while elasticities are higher.

INTRODUCTION

Today it is a well-known fact, established by practical experience, that the rheological properties of polymeric materials are strongly influenced by their molecular weight and its distribution and by the degree of long-chain branching. Therefore, a better understanding of the interrelationships that may exist between the molecular parameters and the rheological properties is very important to both the preparation of new polymers and their processing. However, at present, the theoretical development of this problem is far from complete, though some important progress was made in the 1950s and 1960s by a number of investigators.[1–10]

Experimental studies which relate the rheological properties to the molecular characteristics of polymeric materials have also been reported in the literature. Some investigators[11–20] have studied the effect of the molecular weight and its distribution, and others,[21–25] the effect of the amount of long-chain branching on the rheological properties.

There are, however, some practical difficulties from the experimental point of view in establishing a reliable relationship (or relationships) between the molecular parameters and the rheological properties of a polymer in the *molten* state. One is the accuracy of the experimentally determined molecular weight and its distribution, especially when the polymer has a high molecular weight (say, of the order of a million) and a broad molecular weight distribution, and also when the polymer contains a significant amount of long-chain branching.

Journal of Applied Polymer Science, Vol. 22, 1677–1700 (1978)

0021-8995/78/0022-1677$01.00

Another difficulty is the accuracy of the rheological measurements, especially of the elastic property of a bulk polymer in the molten state at *high* shear rates, say, in the range of 10^2–10^4 sec^{-1} (or *high* shear stresses, say, in the range of 10^5–10^7 dynes/cm^2). It should be noted that the most commonly used polymers in industry exhibit nonlinear behavior in their viscous and elastic properties at high shear rates (or shear stresses), and therefore any attempt at extrapolating the rheological data obtained at low shear rates to high shear rates requires extreme caution, to say the least.

On the other hand, from the point of view of polymer processing operations (e.g., injection molding, fiber spinning, film extrusion), one is extremely interested in relating processability of a polymer to its molecular characteristics; and therefore the measurement of the viscoelastic properties of polymer melts at high shear rates is of fundamental and practical importance.

In this paper, we present our rheological measurements recently made of several commercially available polyethylenes at high shear rates. The study concerns the influence of the molecular weight and its distribution and of the degree of long-chain branching on the viscoelastic properties of polyethylene melts.

EXPERIMENTAL

The apparatus used for the rheological measurements was the capillary rheometer,[26] which provides measurements of wall normal stresses along the die axis. The capillary die used has a length-to-diameter (L/D) ratio of 20 (D = 0.125 in.) and a reservoir-to-capillary diameter (D_R/D) ratio of 16. Details of the die design and experimental procedure, together with some precautions one should take in the use of the capillary rheometer, are described in earlier publications of Han.[26–28]

The materials investigated were three low-density polyethylenes of Chemplex Corp., three low-density polyethylenes of U.S. Industrial Chemicals Co., two high-density polyethylenes of Mitsui Petrochemical Industries, Ltd., and two

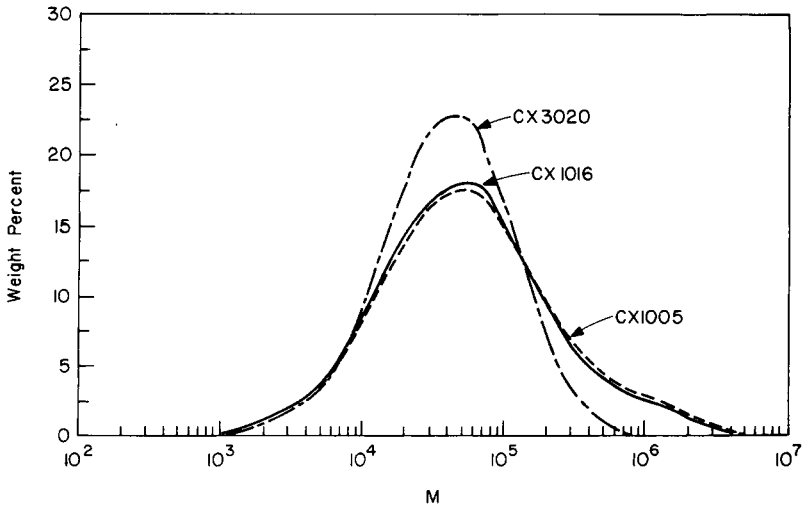

Fig. 1. Molecular weight distribution curves for Chemplex low-density polyethylenes.

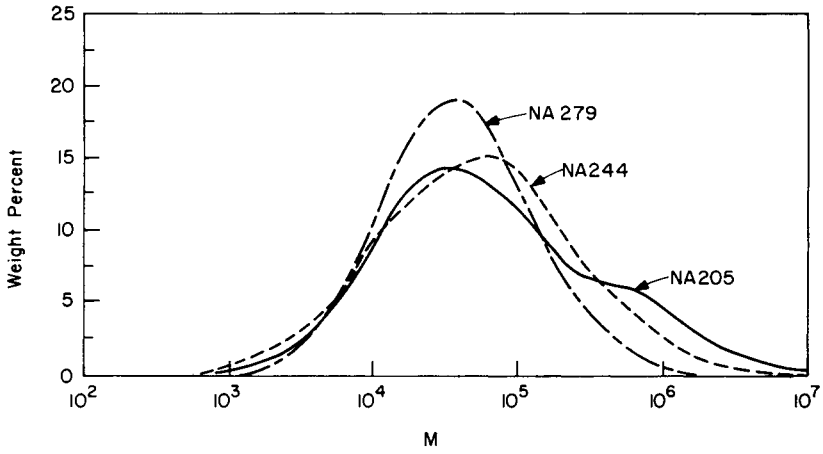

Fig. 2. Molecular weight distribution curves for U.S. Industrial Chemical low-density polyethylenes.

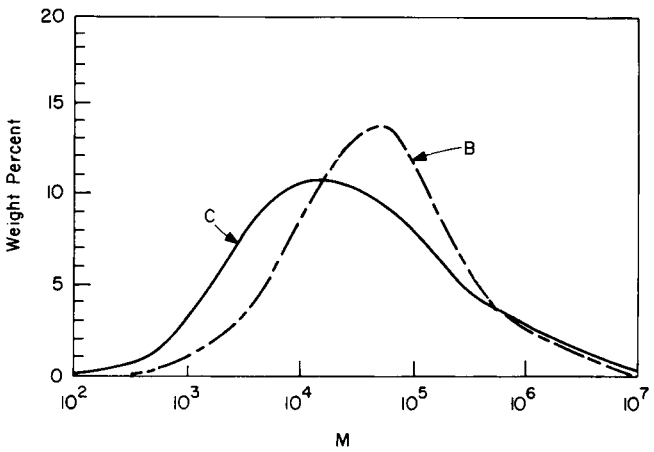

Fig. 3. Molecular weight distribution curves for Mitsui Petrochemical high-density polyethylenes.

high-density polyethylenes of Union Carbide Corp. The molecular weight distribution curves of these samples are given in Figures 1–4, and the average molecular weights of these samples are given in Table I, which were determined by the resin suppliers, using the gel permeation chromatograph (GPC).

THEORETICAL BACKGROUND FOR THE ANALYSIS OF EXPERIMENTAL DATA FROM CAPILLARY FLOW

When pressures (more precisely stated, wall normal stresses) are measured in the reservoir and in the capillary tube, one obtains pressure profiles as shown schematically in Figure 5.[27,28] Two things are worth noting in this figure. One is the exceedingly large pressure drop at the entry to the die section, termed ΔP_{ent} in the figure. The other is the *nonzero* gauge pressure, called the "exit pressure," termed P_{exit}, occurring when the straight-line portion of the pressure profiles is extrapolated to the exit of the die. In the past, numerous researchers, notably

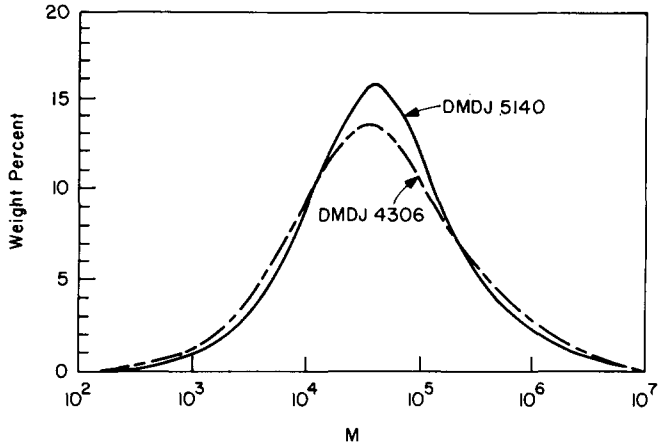

Fig. 4. Molecular weight distribution curves for Union Carbide high-density polyethylenes.

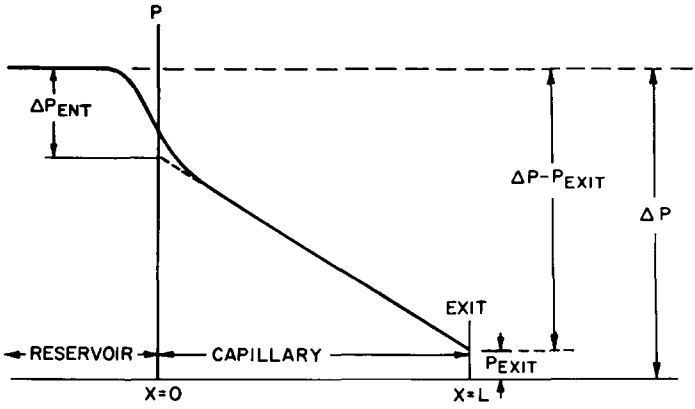

Fig. 5. Schematic diagram of the pressure distribution, both in the reservoir and in the capillary.

Han and coworkers,[26,27,29,30] have discussed the rheological implications of the entrance pressure drop and exit pressure, and the reader may consult the recent monograph by Han.[28]

One of the rheological variables that are of fundamental and practical importance is the shear viscosity η defined by

$$\eta = \tau_w/\dot{\gamma} \tag{1}$$

in which τ_w is the wall shear stres. τ_w may be calculated from the capillary flow experiment using the expression

$$\tau_w = \left(\frac{-\partial p}{\partial z}\right)\frac{R}{2} \tag{2}$$

where R is the capillary radius and $-\partial p/\partial z$ is the pressure gradient, that is, the slope of the pressure profile, which is constant in the fully developed flow regime (see Fig. 5). In eq. (1), $\dot{\gamma}$ is the true wall shear rate defined by

$$\dot{\gamma} = \left(\frac{3n+1}{4n}\right)\dot{\gamma}_{app} \tag{3}$$

in which $\dot{\gamma}_{app}$ and n are defined by

$$\dot{\gamma}_{app} = \frac{4Q}{\pi R^3} \tag{4}$$

TABLE I
Molecular Characteristics of the Polyethylenes Investigated

Polymer	Manufacturer	Sample code	$\overline{M}_n \times 10^{-4}$	$\overline{M}_w \times 10^{-5}$	$\overline{M}_w/\overline{M}_n$	Remarks on the long-chain branching (LCB) frequency
Low-density polyethylene	Chemplex	CX 1005	2.07	1.59	7.69	High
		CX 1016	2.03	1.59	7.85	High
		CX 3020	1.82	0.56	3.08	Low[a]
Low-density polyethylene	U.S. Industrial Chemicals	NA 205	1.89	2.82	14.9	1.12×10^{-4}
		NA 244	1.74	1.53	8.8	0.88×10^{-4}
		NA 279	2.00	0.86	4.3	0.59×10^{-4}
High-density polyethylene	Mitsui Petrochemicals	B	1.25	2.43	19.5	Little branching
		C	0.48	2.26	47.5	Little branching
High-density polyethylene	Union Carbide	DMDJ 5140	1.33	1.74	13.1	Little branching
		DMDJ 4306	0.98	2.12	21.7	Little branching

[a] LCB level is substantially less in CX 3020 than in either CX 1016 or CX 1005, and LCB level between CX 1005 and CX 1016 is not very different.

and

$$n = \frac{d \ln \tau_w}{d \ln \dot{\gamma}_{app}} \tag{5}$$

respectively, and Q denotes the volumetric flow rate.

Other rheological variables that may be obtained from the capillary flow experiment are the normal stress differences[28]:

$$\tau_{11} - \tau_{22} = P_{exit} + \tau_w \frac{dP_{exit}}{d\tau_w} \tag{6}$$

$$\tau_{22} - \tau_{33} = -\tau_w \frac{dP_{exit}}{d\tau_w} \tag{7}$$

in which P_{exit} is the exit pressure obtained by extrapolating the pressure readings to the exit of the die. It should be pointed out that normal stress differences are identically zero for *Newtonian* fluids, and therefore they are conveniently used as a measure of fluid elasticity. Note that viscoelasticity is better defined in terms of memory, and then normal stresses will naturally follow.[28]

The most significant result of all in the use of capillary flow data as described above is that it permits one to determine normal stress differences at high shear rates.

RESULTS AN DISCUSSION

Viscoelastic Behavior of Low-Density Polyethylene Melts

Figure 6 gives plots of viscosity η versus shear rate $\dot{\gamma}$ for the three Chemplex low-density polyethylenes (LDPE) at 180°C, and Figure 7 gives similar plots for the three U.S. Industrial Chemicals LDPEs at 180°C. Space limitations here do not permit us to present viscosity plots at other melt temperatures.

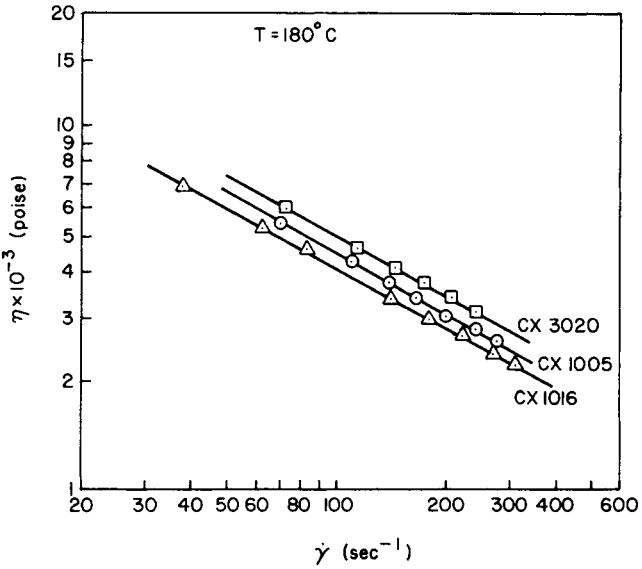

Fig. 6. Viscosity vs shear rate for Chemplex low-density polyethylenes.

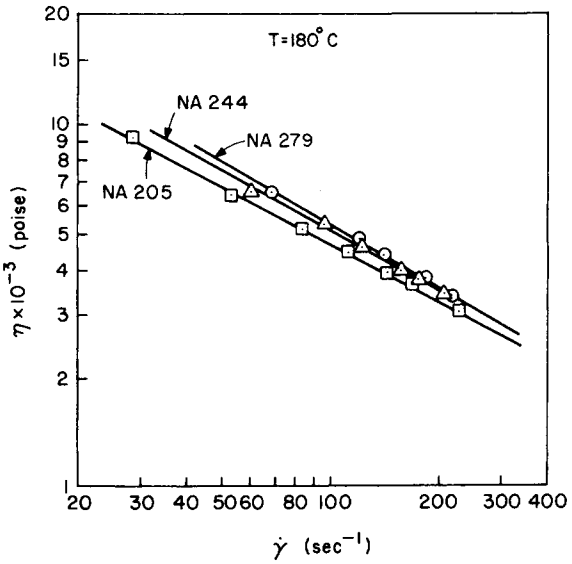

Fig. 7. Viscosity vs shear rate for U.S. Ind. Chemical low-density polyethylenes.

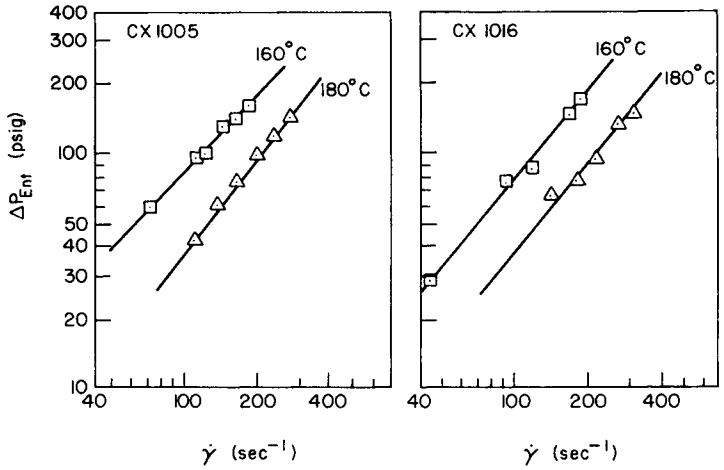

Fig. 8. Entrance pressure drop vs shear rate for Chemplex low-density polyethylenes.

It is seen in Figures 6 and 7 that, over the range of shear rates investigated, viscosity decreases with shear rate, following the power law relation

$$\eta = K\dot{\gamma}^{n-1} \tag{8}$$

Note that the values of n are less than unity for all the materials tested, which is typical of thermoplastic resins.

From the point of view of molecular weight distribution (MWD), there is a clear trend that the materials of narrow MWD have higher viscosities than those of broad MWD. (See Table I and Figs. 1 and 2.) It should be pointed out, however, that the accurate determination of the molecular weight distribution of LDPE by GPC, in the presence of an appreciable amount of long-chain branching, is very difficult, if not impossible. Note further that the MWD curves of CX 1005, CX 1016, and CX 3020 in Figure 1 are constructed on the basis of the linear

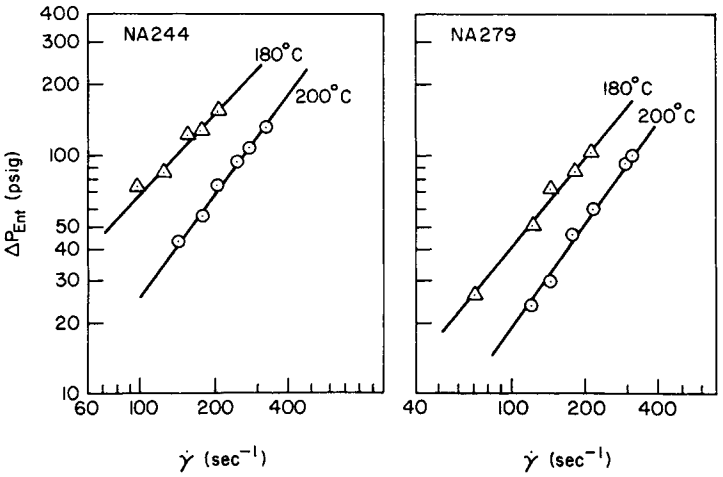

Fig. 9. Entrance pressure drop vs shear rate for U.S. Ind. Chemical low-density polyethylenes.

polyethylene calibration curve, without making corrections for the nonlinearity present in the LDPE having long-chain branching. Therefore, the differences in the average molecular weight (see Table I) and MWD curves (see Fig. 1) between CX 1005 and CX 1016 should not be considered seriously.

Figure 8 gives plots of entrance pressure drop ΔP_{ent} versus shear rate $\dot{\gamma}$ for the Chemplex LDPES at 160° and 180°C, and Figure 9 gives similar plots of the U.S. Industrial Chemicals LDPEs at 180° and 200°C. It is seen that the entrance pressure drop decreases as the melt temperature is increased. However, as may be seen in Figures 10 and 11, plots of entrance pressure drop versus wall shear stress do not show temperature dependence. Now, Figure 12 shows plots of ΔP_{ent} versus τ_w for the three Chemplex LDPEs, and Figure 13 shows similar plots for the three U.S. Industrial Chemicals LDPEs. A clear trend is seen in Figures 12 and 13 that the material of broad MWD gives rise to greater entrance pressure drops than that of narrow MWD (see Table I and Figs. 1 and 2).

It has been known for a long time that when viscoelastic fluids flow from a

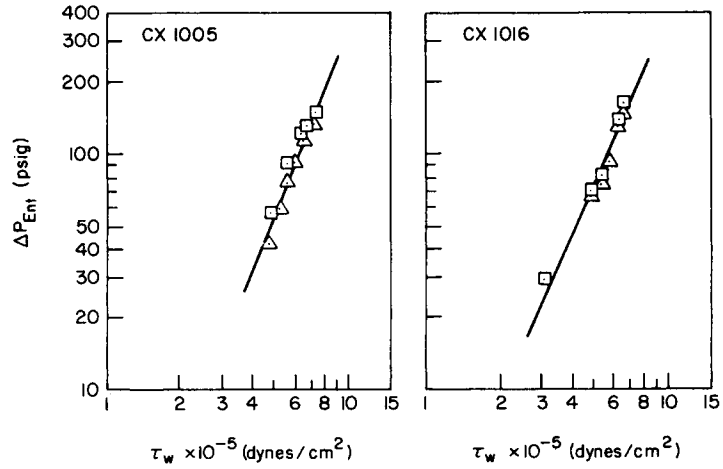

Fig. 10. Entrance pressure drop vs shear stress for Chemplex low-density polyethylenes: (⊡) 160°C; (△) 180°C.

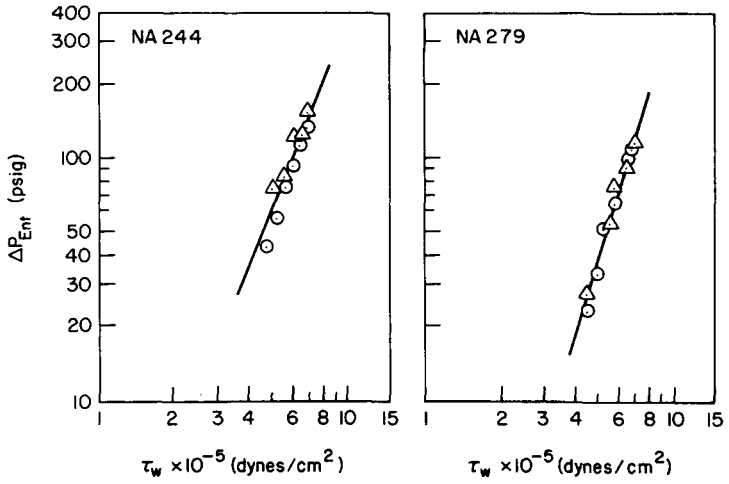

Fig. 11. Entrance pressure drop vs shear stress for U.S. Ind. Chemical low-density polyethylenes: (△) 180°C; (○) 200°C.

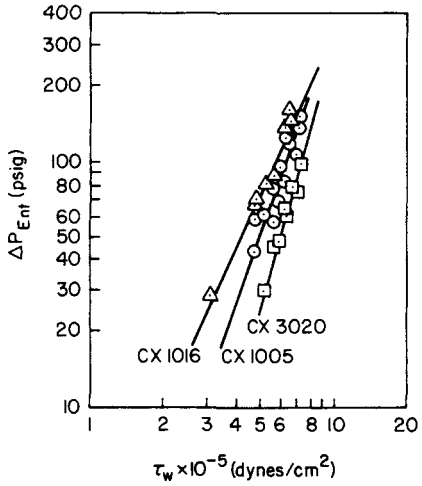

Fig. 12. Entrance pressure drop vs shear stress for Chemplex low-density polyethylenes.

reservoir into a circular tube, they undergo large pressure drops. And some efforts have been made to explain these entrance pressure drops in terms of the elastic properties of the material.[29–34] Today, it is generally agreed among researchers that the great part of the entrance pressure drop may be attributable to the fluid elasticity rather than to the fluid viscosity. It should be mentioned, however, that although the entrance pressure drop may be used as a measure of fluid elasticity for the sake of convenience, it should not be construed as representing the amount of elastic energy stored permanently in the fluid. This is because the elastic energy stored in the entrance region is partially dissipated after the fluid enters the tube, reaching a steady value that is converted to completely recoverable elastic energy. It should be noted further that the flow in the entrance region is *not* a steady, fully developed one. It is an accelerative flow and may be considered as an *unsteady* flow in the Lagrangian sense. Therefore, one should be warned *not* to try to relate the entrance pressure drop

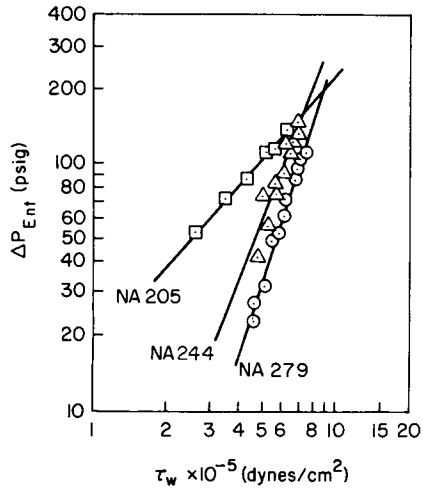

Fig. 13. Entrance pressure drop vs shear stress for U.S. Ind. Chemical low-density polyethylenes.

defined in the converging (nonviscometric) flow field to the normal stress difference defined in the fully developed (viscometric) flow field.

Figure 14 gives plots of exit pressure P_{exit} versus shear rate $\dot{\gamma}$ for a Chemplex LDPE, CX 1016, at three melt temperatures—160°, 180°, and 200°C, and Figure 15 shows similar plots for a U.S. Industrial Chemicals LDPE, NA 244, at 180° and 200°C. It is seen that the exit pressure decreases as the melt temperature is increased. However, as may be seen in Figures 16 and 17, plots of exit pressure versus shear stress do not show temperature dependence, consistent with earlier findings.[28] This observation is very similar to that observed above with respect to the entrance pressure drops. (Compare Figs. 16 and 17 with Figs. 10 and 11.) Now, Figure 18 shows plots of P_{exit} versus τ_w for the three Chemplex LDPEs, and Figure 19 shows similar plots for the three U.S. Industrial Chemicals LDPEs. Again, a clear trend is seen in Figures 18 and 19 that the material of broad MWD gives rise to greater exit pressures than that of narrow MWD, very similar to the

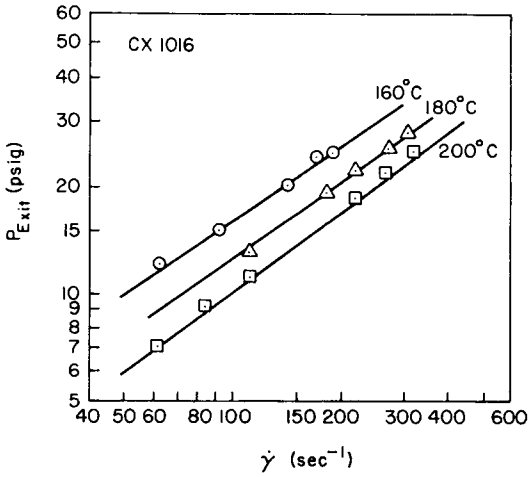

Fig. 14. Exit pressure vs shear rate for Chemplex low-density polyethylene.

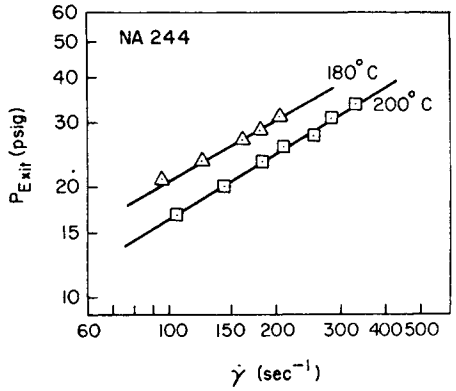

Fig. 15. Exit pressure vs shear rate for U.S. Ind. Chemical low-density polyethylene.

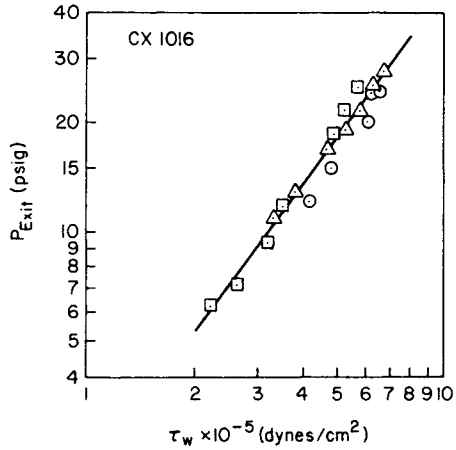

Fig. 16. Exit pressure vs shear stress for Chemplex low-density polyethylene: (⊙) 160°C; (△) 180°C; (⊡) 200°C.

observations made with respect to the entrance pressure drops (compare Figs. 18 and 19 with Figs. 12 and 13).

Using eq. (6), the first normal stress difference $\tau_{11} - \tau_{22}$ is calculated from the plots of exit pressure P_{exit} versus shear stress τ_w, and plots of $\tau_{11} - \tau_{22}$ versus τ_w are given in Figure 20 for the three Chemplex LDPEs, and in Figure 21 for the three U.S. Industrial Chemicals LDPEs. Note that plots of $\tau_{11} - \tau_{22}$ versus τ_w are independent of melt temperature, and therfore such plots may be used for comparing the melt elasticity of one material against that of another.

At the exit region of a die, the extrudate swells give rise to an extrudate diameter d_j greater than the tube diameter D. The ratio d_j/D is called the die swell ratio, and it is, of course, greater than unity. The die swell ratio is found to be a function of the throughput rate (and hence shear rate) for a specific tube and a given polymer. Figure 22 gives plots of die swell ratio d_j/D versus shear rate $\dot{\gamma}$ for a Chemplex LDPE, CX 1005, at three melt temperatures—160°, 180°, and 200°C. It is seen that the die swell ratio decreases as the melt temperature is increased. However, plots of d_j/D versus wall shear stress τ_w become independent of temperature, as may be seen in Figure 23 for the three Chemplex LDPEs, and in Figure 24 for the three U.S. Industrial Chemicals LDPEs. Once

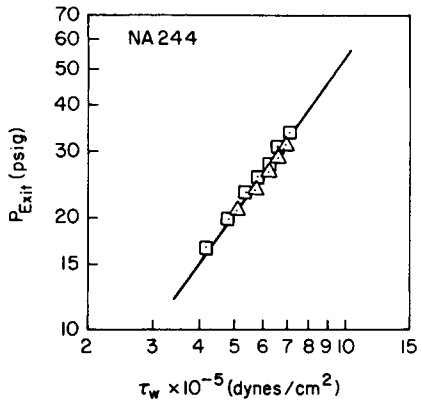

Fig. 17. Exit pressure versus shear stress for U.S. Ind. Chemical low-density polyethylene: (△) 180°C; (⊡) 200°C.

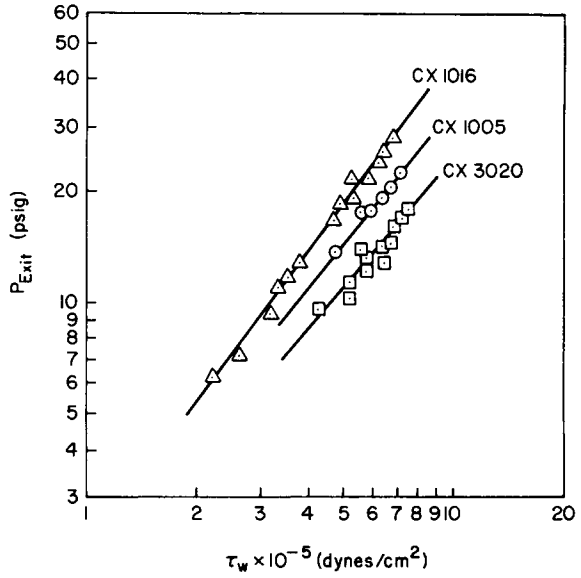

Fig. 18. Exit pressure vs shear stress for Chemplex low-density polyethylenes.

again, a clear trend is seen that the material of broad MWD gives rise to greater die swell than that of narrow MWD (see Table I and Figs. 1 and 2).

The swelling of extrudate has also been attributed to the elasticity of the fluid, and several researchers[35–37] have attempted to relate the die swell ratio theoretically to the first normal stress difference. From the rheological point of view, it is believed that die swell occurs as a result of the recovery of the elastic deformation imposed in the capillary. In other words, should there be *no* elastic energy to be recovered in the melt at the die exit, then no swelling of the extrudate should be observed upon exiting from a capillary. According to Han,[26,30] the exit pressure (more precisely stated, the wall normal stress at the exit plane) indeed represents the amount of the elastic energy recoverable in the melt at the die exit. On the basis of this contention, the existence of both die swell and exit pressure must have the same physical origin, and therefore there ought to be a correlation between the two. This indeed can be observed from Figures 25 and 26. A similar observation was also reported earlier.[38]

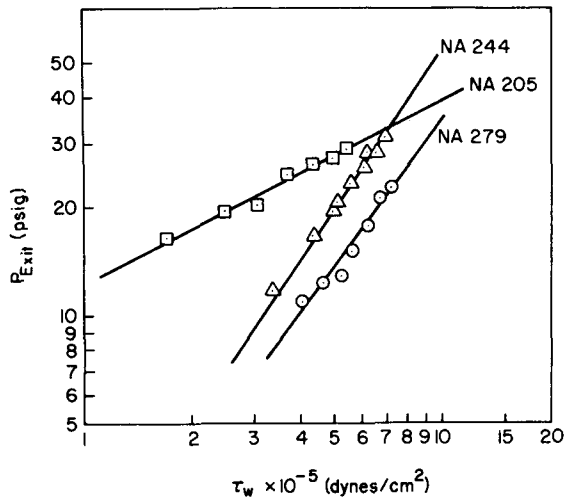

Fig. 19. Exit pressure vs shear stress for U.S. Ind. Chemical low-density polyethylenes.

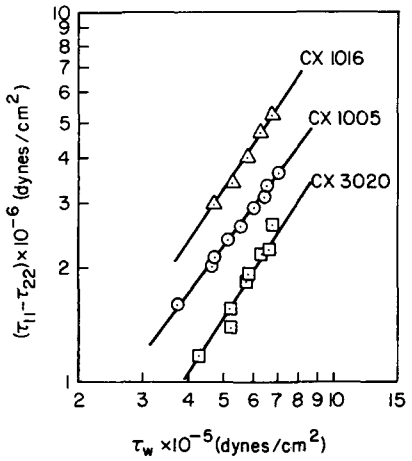

Fig. 20. Normal stress difference vs shear stress for Chemplex low-density polyethylenes.

Of particular interest in the results presented above is the similarity in the behavior of entrance pressure drop ΔP_{ent}, exit pressure P_{exit}, die swell ratio d_j/D, and normal stress difference $\tau_{11} - \tau_{22}$ when they are plotted against shear stress (see Figs. 12, 13, 18–21, 23, and 24).

It should be noted that the extrapolation made to obtain the exit pressure from the wall normal stress measurements assumes that, as the melt approaches the exit plane of the die, velocity rearrangement is negligible and therefore that extrapolating pressure readings to the exit of the die is valid. A test of this assumption by means of some direct experimental technique is very crucial. Han and Drexler[39] tested the assumption experimentally by measuring stress-birefringent patterns of flowing melts at the exit region of a slit die, and they indeed found that the disturbance of stresses at the exit plane is negligibly small, at least for polymer melts at reasonably high shear rates, say, greater than 10 sec^{-1}.

To be useful for further rheological investigations, measurements of die swell ratio must be correlatable with normal stress differences. In this context, several

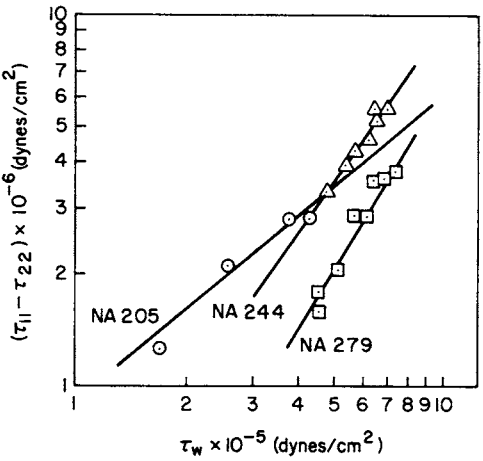

Fig. 21. Normal stress difference vs shear stress for U.S. Ind. Chemical low-density polyethylenes.

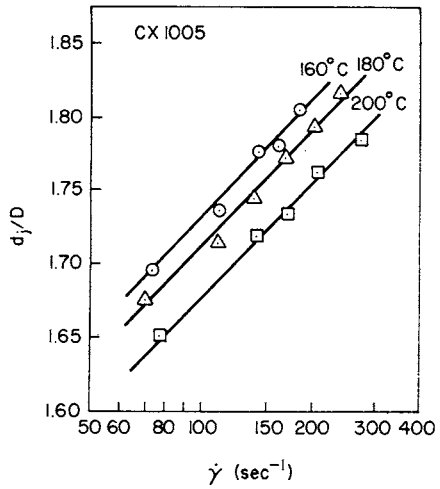

Fig. 22. Die swell ratio vs shear rate for Chemplex low-density polyethylene.

investigators have made attempts to relate the die swell ratio to the first normal stress difference by using the concept of unconstrained elastic recovery.[35–37] Table II summarizes three theoretical expressions that relate the first normal stress difference $N_1 = \tau_{11} - \tau_{22}$ to the die swell ratio d_j/D, and Table III gives values of N_1 calculated for various theories, using die swell data and exit pressure data of the low-density polyethylenes investigated. It is seen that they all give comparable orders of magnitude of the first normal stress difference in polymer melt flow.

Viscoelastic Behavior of High-Density Polyethylene Melts

Figures 27 and 28 give plots of viscosity η and first normal stress difference $\tau_{11} - \tau_{22}$ versus shear rate $\dot{\gamma}$ for resin B and resin C, respectively. These resins are Mitsui high-density polyethylenes. It is seen that, over the range of shear rates investigated, viscosity decreases with shear rate, following a power law

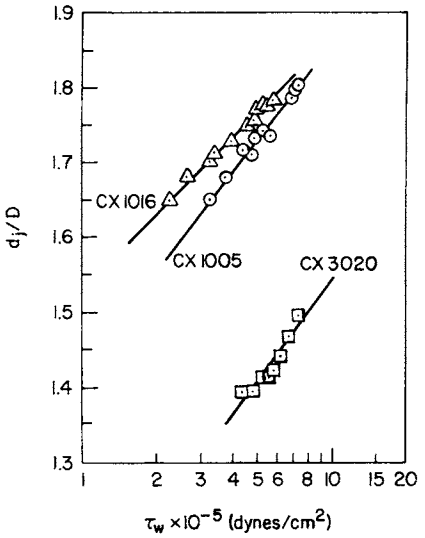

Fig. 23. Die swell ratio vs shear stress for Chemplex low-density polyethylenes.

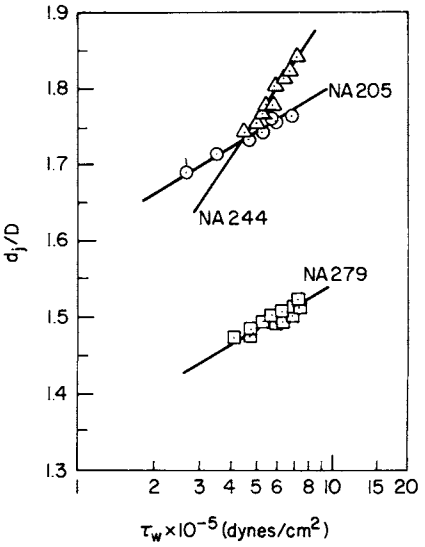

Fig. 24. Die swell ratio vs shear stress for U.S. Ind. Chemical low-density polyethylenes.

relation, eq. (8), and that normal stress difference increases with shear rate. Note that an increase in melt temperature brings about a decrease in both viscosity and normal stress difference.

For comparison purposes, plots of η versus $\dot{\gamma}$ are given in Figure 29, and plots of $\tau_{11} - \tau_{22}$ versus τ_w are given in Figure 30 for both resins B and C at 250°C. It is seen in Figures 29 and 30 that resin B, having a narrow MWD, has at the same time higher viscosities and lower elasticities than resin C, which has a broad MWD (see Table I and Fig. 3).

Figures 31 and 32 give plots of viscosity η and first normal stress difference $\tau_{11} - \tau_{22}$ versus shear rate $\dot{\gamma}$ for resin DMDJ 5140 and resin DMDJ 4306, respectively. These are Union Carbide high-density polyethylenes. It is seen that,

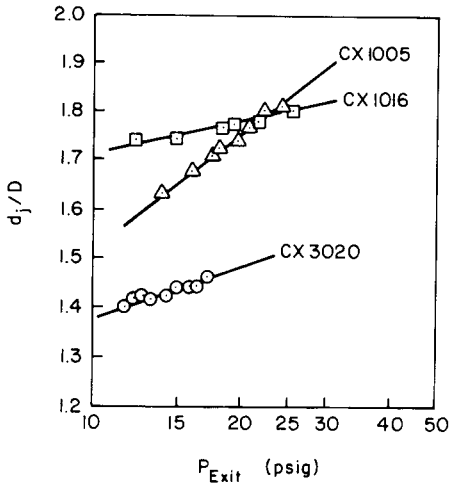

Fig. 25. Die swell ratio vs exit pressure for Chemplex low-density polyethylenes.

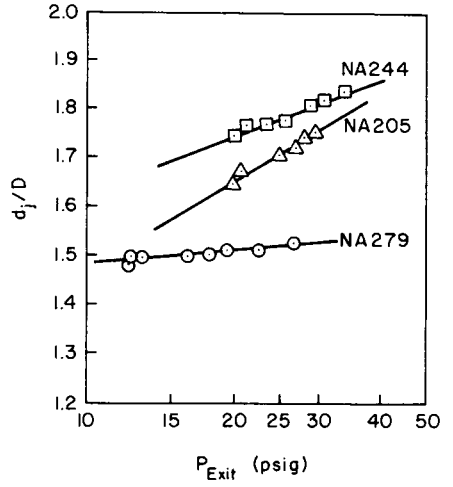

Fig. 26. Die swell ratio vs exit pressure for U.S. Ind. Chemical low-density polyethylenes.

over the range of shear rates investigated, η decreases and $\tau_{11} - \tau_{22}$ increases as $\dot{\gamma}$ is increased, behavior that is very similar to that observed for the several LDPE resins and the Mitsui HDPE resins discussed above.

For comparison purposes, plots of η versus $\dot{\gamma}$ are given in Figure 33, plots of $\tau_{11} - \tau_{22}$ versus τ_w are given in and Figure 34 for both resins DMDJ 5140 and DMDJ 4306 at 240°C. It is seen in these figures that resin DMDJ 5140, with a narrow MWD, has higher viscosities and lower elasticities than resin DMDJ 4306, which has a broad MWD (see Table I and Fig. 4).

Molecular Interpretation of Rheological Measurements

In the past, some theoretical attempts have been made to take into account the effect of the molecular weight distribution on the variation of viscosity. Middleman[40] has suggested a method of constructing master viscosity curves with polydispersity as a parameter by extending the Bueche theory.[41] According

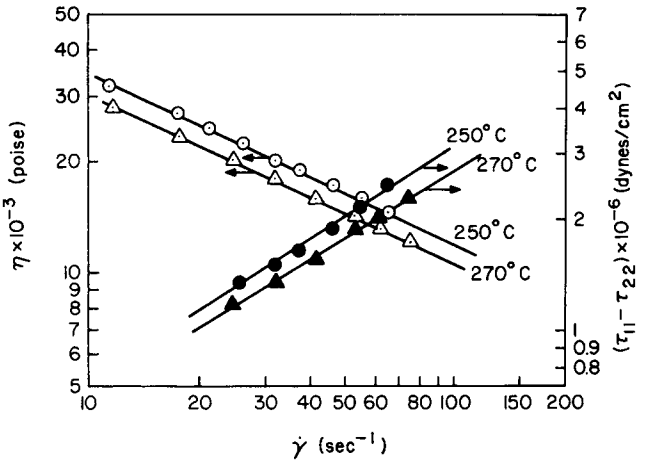

Fig. 27. Viscosity and normal stress difference vs shear rate for Mitsui high-density polyethylene, resin B.

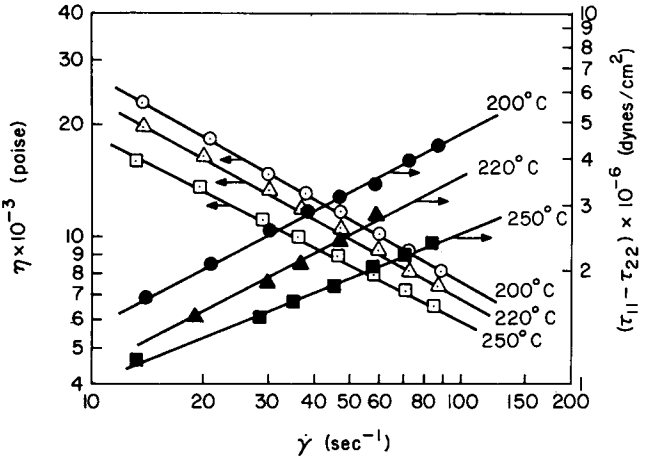

Fig. 28. Viscosity and normal stress difference vs shear rate for Mitsui high-density polyethylene, resin C.

TABLE II
Summary of Theoretical Expressions of $\tau_{11} - \tau_{22}$ from Die Swell Data[28]

Investigator	$\tau_{11} - \tau_{22}$
Bagley and Duffey[35]	$2\tau_w[(d_j/D)^4 - (d_j/D)^{-2}]^{1/2}$
Graessley et al.[36]	$2^{1/2}\tau_w[(d_j/D)^4 - (d_j/D)^{-2}]^{1/2}$
Tanner[37]	$2\tau_w[2(d_j/D)^6 - 2]^{1/2}$

to Bueche,[41,42] a polymer molecule is to be divided into a large number of submolecules each of which behaves like a small mass attached to a linear spring.

Graessley and Segal[15] have also suggested a method of constructing master viscosity curves by applying the molecular entanglement theory.[9] In the Graessley theory, the decrease in viscosity with shear rate in the non-Newtonian regime is viewed as a consequence of the net decrease in entanglement density induced by flow.

TABLE III
Comparison of the Theoretically Predicted Values of Normal Stress Differences from Various Die Swell Theories and Han Exit Pressure Theory

$\dot{\gamma}$, sec^{-1}	d_j/D	P_{exit}, psig	N_1, dynes/cm^2, from die swell theory: Bagley-Duffey[35]	Graessley et al.[36]	Tanner[37]	N_1, dynes/cm^2, from Han exit pressure theory[27]
			a. CX1005 at 180°C			
111.4	1.712	17.52	2.68×10^6	1.89×10^6	6.49×10^6	2.03×10^6
139.2	1.745	19.67	3.08×10^6	2.17×10^6	7.57×10^6	2.41×10^6
169.0	1.774	20.54	3.45×10^6	2.44×10^6	8.66×10^6	2.64×10^6
202.6	1.793	22.13	3.83×10^6	2.71×10^6	9.71×10^6	2.97×10^6
239.9	1.816	24.44	4.25×10^6	3.01×10^6	10.91×10^6	3.43×10^6
			b. CX1016 at 180°C			
110.9	1.752	12.81	2.73×10^6	1.93×10^6	6.77×10^6	2.07×10^6
181.6	1.771	19.25	3.30×10^6	2.33×10^6	8.25×10^6	3.45×10^6
222.7	1.780	21.79	3.63×10^6	2.57×10^6	9.19×10^6	4.02×10^6
269.6	1.789	25.53	3.97×10^6	2.81×10^6	10.04×10^6	4.77×10^6
			c. CX3020 at 180°C			
115.5	1.404	11.64	1.94×10^6	1.37×10^6	3.84×10^6	1.59×10^6
145.3	1.413	13.30	2.18×10^6	1.56×10^6	4.35×10^6	1.96×10^6
175.1	1.426	14.14	2.45×10^6	1.73×10^6	4.94×10^6	2.25×10^6
204.0	1.441	16.32	2.68×10^6	1.89×10^6	5.46×10^6	2.74×10^6
243.2	1.461	18.09	3.00×10^6	2.12×10^6	6.20×10^6	3.26×10^6

			d. NA205 at 200°C			
67.2	1.683	20.48	1.76×10^6	1.24×10^6	4.18×10^6	2.30×10^6
101.9	1.713	25.29	2.02×10^6	1.53×10^6	5.23×10^6	2.82×10^6
137.1	1.734	27.06	2.63×10^6	1.86×10^6	6.44×10^6	2.96×10^6
			e. NA244 at 200°C			
142.1	1.754	20.08	2.92×10^6	2.07×10^6	7.25×10^6	3.38×10^6
179.4	1.780	23.52	3.36×10^6	2.38×10^6	8.46×10^6	3.96×10^6
206.8	1.806	25.84	3.70×10^6	2.53×10^6	9.45×10^6	4.35×10^6
250.9	1.815	27.97	4.02×10^6	2.84×10^6	10.31×10^6	4.70×10^6
280.3	1.823	30.85	4.28×10^6	3.03×10^6	11.03×10^6	5.11×10^6
328.3	1.845	33.92	4.67×10^6	3.30×10^6	12.17×10^6	5.67×10^6
			f. NA279 at 180°C			
70.5	1.479	6.22	1.98×10^6	1.40×10^6	4.04×10^6	1.78×10^6
144.1	1.496	12.50	2.65×10^6	1.87×10^6	5.61×10^6	2.88×10^6
184.4	1.505	17.98	2.97×10^6	2.10×10^6	6.31×10^6	3.76×10^6
219.7	1.513	19.56	3.20×10^6	2.27×10^6	6.86×10^6	3.81×10^6

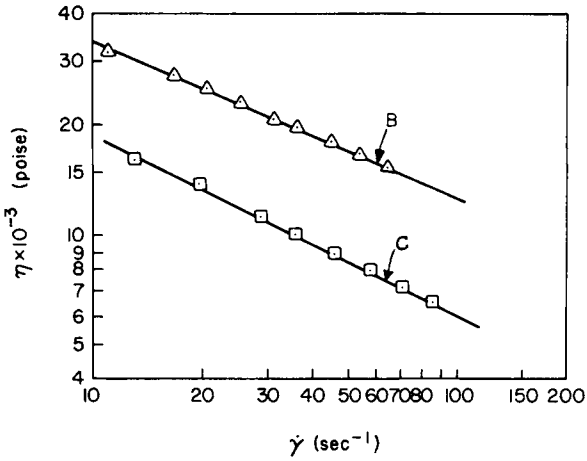

Fig. 29. Viscosity vs shear rate for Mitsui high-density polyethylenes, resins B and C, at 250°C.

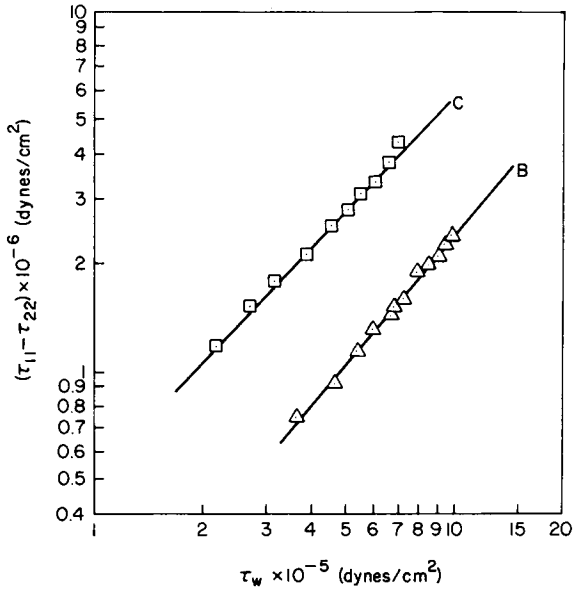

Fig. 30. Normal stress difference vs shear stress for Mitsui high-density polyethylenes, resins B and C.

The dependence of steady shear viscosity on MWD, as evidenced by the experimental results presented above (see Figs. 6, 7, 29, and 33) is entirely consistent with the theories of Middleman[40] and Graessley and Segal,[15] predicting that the melt viscosity is less for polymers having a broad MWD than for polymers having a narrow MWD. Guillet et al.[23] attribute this to the greater degree of chain entanglement that occurs with a broad distribution of molecular weight. The findings of the present investigation are in agreement with earlier findings of other investigators.[12–18]

It should be noted that a comparison of fluid viscosities of two or more polymers must be made at the same value of either the number-average molecular weight $\overline{M}_n$ or the weight-average molecular weight $\overline{M}_w$. Earlier, Ballman and

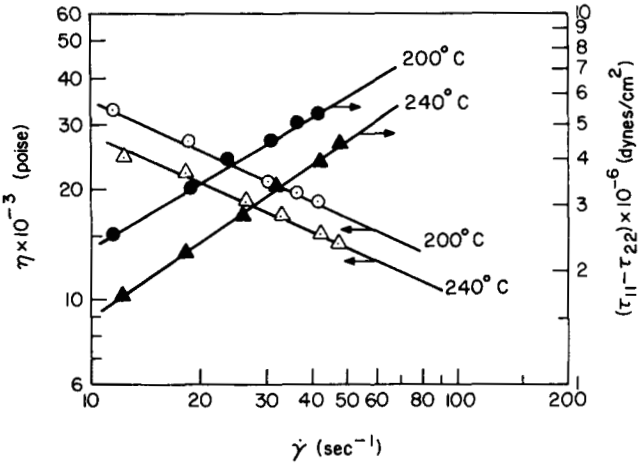

Fig. 31. Viscosity and normal stress difference vs shear rate for Union Carbide high-density polyethylene, resin DMDJ 5140.

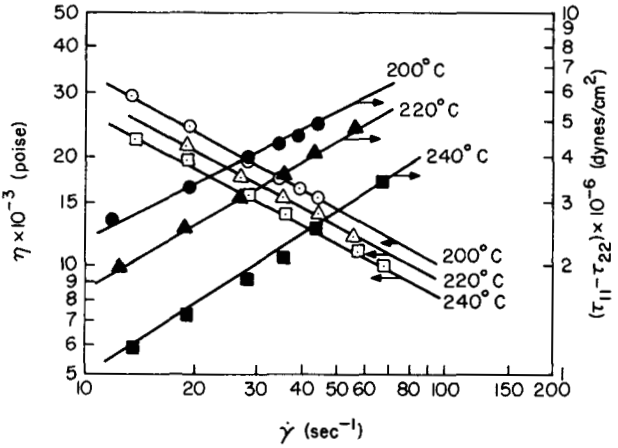

Fig. 32. Viscosity and normal stress difference vs shear rate for Union Carbide high-density polyethylene, resin DMDJ 4306.

Simon[43] concluded from their study that the melt viscosity depends on the $\overline{M}_w$ at low shear rates and on the $\overline{M}_n$ at high shear rates.

Let us now look for a molecular interpretation of the dependence of fluid elasticity on MWD. Elastic recovery, for instance, has long been considered a useful parameter for determining the fluid elasticity. If is often referred to as a measure of stored elastic energy and is characterized by the steady-state elastic compliance J_e defined as

$$J_e = (\tau_{11} - \tau_{22})/2\tau_w{}^2 \tag{9}$$

Note that in principle eq. (9) is valid only at low shear stresses, where $\tau_{11} - \tau_{22}$ is proportional to the square of τ_w.

From the molecular point of view, Ferry et al.[44] have shown that for a polydisperse polymer, J_e may be represented in terms of the average molecular weights by

$$J_e = (2/5\rho RT)(\overline{M}_z\overline{M}_{z+1}/\overline{M}_w) \tag{10}$$

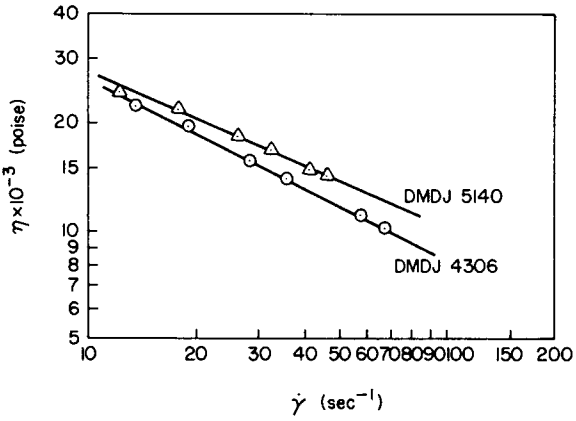

Fig. 33. Viscosity vs shear rate for Union Carbide high-density polyethylenes, resins DMDJ 5140 and DMDJ 4306, at 240°C.

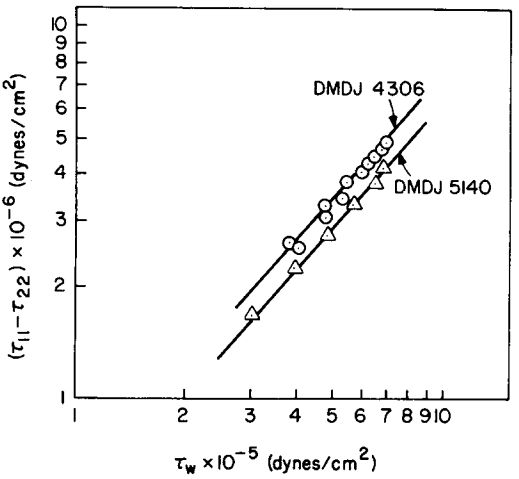

Fig. 34. Normal stress difference vs shear stress for Union Carbide high-density polyethylenes, resins DMDJ 5140 and DMDJ 4306.

where ρ is the fluid density, R is the gas constant, T is the temperature, and $\overline{M}_z$ and $\overline{M}_{z+1}$ are the z-average and $(z + 1)$-average molecular weights, respectively. The rheological significance of eq. (10) is that the steady-state elastic compliance J_e should increase with spread of molecular weight distribution; that is, the fluid elasticity is greater for polymers having a broad MWD than polymers having a narrow MWD.

We can now see that the findings of the present investigation (e.g., plots of $\tau_{11} - \tau_{22}$ versus τ_w given in Figs. 20, 21, 30, and 34) are consistent with the molecular interpretation given by eq. (10). Earlier, other researchers[13,14,18,23] also reported their experimental findings that the fluid elasticity increases as the MWD broadens.

It has long been recognized that the degree of long-chain branching (LCB) influences both the viscous and the elastic behavior of low-density polyethylene. A close examination of Table I reveals that in both the Chemplex and U.S. Industrial Chemicals LDPEs, the number-average molecular weight $\overline{M}_n$ is ap-

proximately the same but the weight-average molecular weight $\overline{M}_w$ varies from material to material, and that the degree of LCB is greater in the material having large values of $\overline{M}_w$ (and hence broad MWD) than that in the material having small values of $\overline{M}_w$. It appears then that the degree of LCB is associated with the breadth of the MWD. It can now be concluded from Figures 6, 7, 12, 13, 18–21, 23, and 24 that the polymer having more LCB has lower viscosities and higher elasticities than the polymer having less LCB (see Table I). It is of particular interest to note that the three different measures of fluid elasticity employed in the study, namely, the entrance pressure drop, the exit pressure, and the die swell ratio, all give rise to consistent results. Similar results were reported in earlier publications by other investigators.[45,46]

The authors wish to gratefully acknowledge the supply of the resins employed and the information received of molecular weight measurements (given in Table I and Figs. 1–4) from Chemplex Corp., Mitsui Petrochemical Industries, Ltd., Union Carbide Corp., and U.S. Industrial Chemicals Company. Without the help of these companies, this study would not have been possible.

References

1. P. E. Rouse, Jr., *J. Chem. Phys.*, **21**, 1272 (1953); *ibid.*, **22**, 1570 (1954).
2. F. Bueche, *J. Chem. Phys.*, **22**, 603, 1570 (1954).
3. B. H. Zimm, *J. Chem. Phys.*, **24**, 269 (1956).
4. W. L. Peticolas and J. M. Watkins, *J. Am. Chem. Soc.*, **79**, 5083 (1957).
5. W. L. Peticolas, *J. Chem. Phys.*, **35**, 2128 (1961).
6. W. L. Peticolas, *J. Polym. Sci.*, **58**, 1405 (1962).
7. M. C. Williams, *J. Chem. Phys.*, **42**, 2988 (1965).
8. M. Yamamoto, *J. Phys. Soc.* (Japan) **11**, 413 (1956); *ibid.*, **12**, 1148 (1957).
9. W. W. Graessley, *J. Chem. Phys.*, **43**, 2696 (1965); *ibid.*, **47**, 1942 (1967).
10. W. W. Graessley, *J. Chem. Phys.*, **54**, 5143 (1971).
11. J. D. Ferry, M. L. Williams, and D. M. Stern, *J. Chem. Phys.*, **58**, 987 (1954).
12. J. E. Guillet, R. L. Combs, D. F. Slonaker, D. A. Weemes, and H. W. Coover, *J. Appl. Polym. Sci.*, **9**, 796 (1965).
13. J. W. C. Adamse, H. Janeschitz-Kriegl, J. L. den Otter, and J. L. S. Wales, *J. Polym. Sci. A-2*, **6**, 871 (1968).
14. R. L. Combs, D. F. Slonaker, and H. W. Coover, *J. Appl. Polym. Sci.*, **13**, 519 (1969).
15. W. W. Graessley and L. Segal, *A.I.Ch.E. J.*, **16**, 261 (1970).
16. H. Endo, T. Fujimoto, and M. Nagasawa, *J. Polym. Sci. A-2*, **9**, 345 (1971).
17. D. P. Thomas, *Polym. Eng. Sci.*, **11**, 305 (1971).
18. C. D. Han, T. C. Yu, and K. U. Kim, *J. Appl. Polym. Sci.*, **15**, 1149 (1971).
19. W. C. Uy and W. W. Graessley, *Macromolecules*, **4**, 458 (1971).
20. N. Nishida, D. G. Salladay, and J. L. White, *J. Appl. Polym. Sci.*, **15**, 1181 (1971).
21. A. Charlesby, *J. Polym. Sci.*, **17**, 379 (1955).
22. E. B. Bagley, *J. Appl. Phys.*, **31**, 1126 (1960).
23. J. E. Guillet, R. L. Combs, D. F. Slonaker, D. A. Weems, and H. W. Coover, *J. Appl. Polym. Sci.*, **9**, 757 (1965); *ibid.*, **9**, 767 (1965).
24. W. W. Graessley and J. S. Prentice, *J. Polym. Sci. A-2*, **6**, 1887 (1968).
25. E. S. Shinbach and W. W. Graessley, *ACS Polym.* Prepr., **14** (1), 58 (1973).
26. C. D. Han, T. C. Yu, and K. U. Kim, *J. Appl. Polym. Sci.*, **15**, 1149 (1971).
27. C. D. Han, *Trans. Soc. Rheol.*, **18**, 163 (1974).
28. C. D. Han, *Rheology in Polymer Processing*, Academic Press, New York, 1976.
29. C. D. Han, *A.I.Ch.E. J.*, **17**, 1480 (1971).
30. C. D. Han and K. U. Kim, *Polym. Eng. Sci.*, **11**, 395 (1971).
31. W. Philippoff and F. H. Gaskins, *Trans. Soc. Rheol.*, **2**, 263 (1958).
32. H. L. LaNieve and D. C. Bogue, *J. Appl. Polym. Sci.*, **12**, 353 (1968).
33. T. F. Ballenger and J. L. White, *J. Appl. Polym. Sci.*, **15**, 1949 (1971).
34. T. F. Ballenger, I. J. Chen, J. W. Crowder, G. E. Hagler, D. C. Bogue, and J. L. White, *Trans. Soc. Rheol.*, **15**, 195 (1971).
35. E. B. Bagley and H. J. Duffey, *Trans. Soc. Rheol.*, **14**, 545 (1970).

36. W. W. Graessley, S. D. Glasscock, and R. L. Crawley, *Trans. Soc. Rheol.*, **14,** 519 (1970).
37. R. I. Tanner, *J. Polym. Sci. A-2,* **8,** 2067 (1970).
38. C. D. Han, M. Charles, and W. Philippoff, *Trans. Soc. Rheol.*, **14,** 393 (1970).
39. C. D. Han and L. H. Drexler, *Trans. Soc. Rheol.*, **17,** 659 (1973).
40. S. Middleman, *J. Appl. Polym. Sci.*, **11,** 417 (1967).
41. F. Bueche, *J. Chem. Phys.*, **22,** 1570 (1954).
42. F. Bueche, *J. Chem. Phys.*, **22,** 603 (1954).
43. R. L. Ballman and R. H. M. Simon, *J. Polym. Sci.*, **A2,** 3557 (1964).
44. J. D. Ferry, M. L. Williams, and D. M. Stern, *J. Chem. Phys.*, **58,** 987 (1954).
45. L. Wild, R. Rangrath, and D. Knobelock, paper presented at the 68th A.I.Ch.E. Annual Meeting, Los Ageles, Calif., November 16–20, 1975.
46. M. Shida, R. N. Sharoff, and L. V. Cancio, Paper presented at the 68th A.I.Ch.E. Annual Meeting, Los Angeles, Calif., November 16–20, 1975.

Received February 16, 1977
Revised April 1, 1977